

## OPERATIONAL CHARACTERISTICS OF FLAT PLATE CLOSED LOOP PULSATING HEAT PIPES

Honghai Yang <sup>†</sup>, Sameer Khandekar and Manfred Groll

Institut für Kernenergetik und Energiesysteme,  
Universität Stuttgart, 70569 Stuttgart, Germany

<sup>†</sup> corresponding author: Tel: (+49) 711 685-2479, E-mail: yang@ike.uni-stuttgart.de

### ABSTRACT

Feasibility of flat plate closed loop pulsating heat pipe as an integral heat spreader is studied. The paper presents the results of an experimental study (including visualization) on a device made of aluminum. It consists of 40 channels (20 turns each in the evaporator and the condenser), with square cross section ( $2 \times 2 \text{ mm}^2$ , 165 mm long) machined directly on the aluminum plate ( $180 \times 120 \times 3 \text{ mm}^3$ ) which is covered by a transparent polycarbonate plate. The working fluid employed is ethanol. Some peculiar operational characteristics and trends, in comparison with circular channel devices, are observed which are attributed to the sharp angled corners of the channels. Various flow patterns and their transitions, having profound effect on the thermal performance, are reported and found to be dependent on the fluid filling ratio, input heat load as well as the device orientation. The thermal performance is analyzed under different operating boundary conditions. Successful operation at all orientations with respect to gravity is also achieved.

**KEY WORDS:** flat plate closed loop pulsating heat pipe, flow patterns, operational characteristics, parametric influences.

### 1 INTRODUCTION

There is an ongoing effort to combine electronic components and heat spreaders on the chip level which can substantially contribute towards the contemporary trend for miniaturization. Pulsating heat pipes (PHPs), as proposed by Akachi [1-3] have already found applications in cooling power/microelectronic components but not many studies exist on the feasibility of these devices as integrated heat spreaders. This will necessitate flat plate structures having typical dimensions as applicable for multi-chip modules or printed circuit boards. Another potential application of such PHP plates can be in space based radiator plates for satellite and other similar applications. This seems to be the next logical step for widening the application area of pulsating heat pipes.

This study focuses on flat plate structures with channels of square cross section forming a closed loop structure. Previous studies suggest some interesting thermal behavior of plate PHP structures i.e. inter-channel heat transfer, contact angle hysteresis, capillary effects due to sharp corners, etc. [4]. These and other operational aspects need to be further studied and verified for the acceptability of the technology.

### 2 DESCRIPTION OF EXPERIMENTS

The details of the experimental set-up are shown schematically in Figure 1. The device was made of an aluminum plate ( $180 \times 120 \times 3 \text{ mm}^3$ ) with 40 parallel rectangular channels (20 turns each in the evaporator and the condenser area) milled on it, forming a looped serpentine structure. Channel dimensions were  $165 \times 2 \times 2 \text{ mm}^3$ . A polycarbonate plate with a transparent 'silikon' gasket was used to cover the device from the top for visualization. A copper heater block ( $100 \times 30 \times 15 \text{ mm}^3$ ) having three embedded cartridge heaters (250W each) and a water cooled (always supplied with water at  $20^\circ\text{C}$ ), copper cold plate ( $100 \times 60 \times 12 \text{ mm}^3$ ) were attached on the back face of the aluminum PHP plate. The area between the heater and cold plate forms the adiabatic section. A vacuum/ charging tube was provided in the center of the PHP plate.

Axial temperature distribution was measured by Type-K thermocouples (2 each in evaporator and in the adiabatic section and 3 in the condenser) and recorded by a data logging system. Ethanol was used as the working fluid with filling ratios (liquid volume to the total PHP volume) ranging from dry structure to 90%. The dry structure test served as reference measurement. The set-up could be tilted from vertical bottom heat mode to top heat mode.

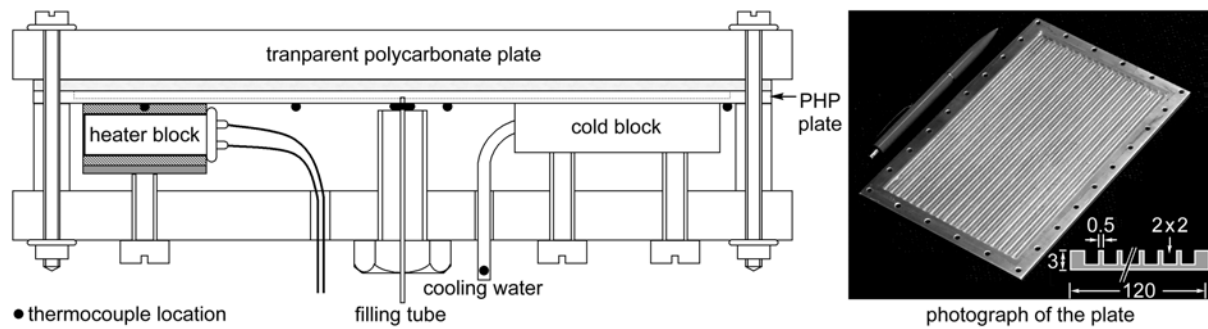


Figure 1: Schematic of the experimental set-up

### 3 RESULTS AND DISCUSSION

#### 3.1 Effect of tube cross section

Before proceeding to the actual results it is worthwhile to discuss the effect of the tube cross section on the operational characteristics of pulsating heat pipes.

Comparing a circular channel of diameter  $D$  and a square section of side =  $D$ , although we notice that the hydraulic diameters of both the geometries are the same ( $= D$ ), the volume per unit length of the latter geometry is  $(4/\pi)$  times the former. Thus, if we make two pulsating heat pipes with circular and square sections having the same hydraulic diameter, there will be a fundamental difference in their operating characteristics.

Referring to Figure 2, if a square cross section channel is filled below about 27.3%, then all the liquid will tend to accumulate in the corners. This gives rise to some capillary action generated due to sharp angled corners. The menisci recede to lower

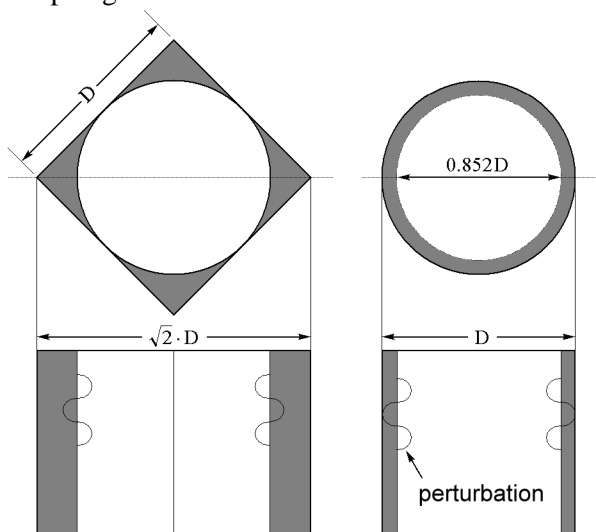


Figure 2: Effect of tube cross section; both tubes have the same hydraulic diameter and both are filled with 27.3% of working fluid

radii of curvature if the filling ratio is made less than 27.3%, improving the capillary action of the sharp corners of the cross section. On the contrary, such a phenomenon is not expected in a circular channel although both have the same hydraulic diameter. If we fill the circular cross section tube with, say 10% liquid, then the probability of distinct liquid plug formation is definitely much higher than for the equivalent square cross section channel (provided the tube diameter is comparable to or less than the critical diameter specified by the critical Bond number criterion). Furthermore, in the background of the ongoing discussion, it is self-evident that the critical diameter governed by the Bond number, as given by Eq. (1) below, is rather inappropriate for the case of channels with sharp angled corners.

$$D_{\text{crit}} \leq 2 \cdot \left[ \frac{\sigma}{(\rho_{\text{liq}} - \rho_{\text{vap}}) \cdot g} \right]^{0.5} \quad (1)$$

The shape also affects the flow regime transitions. The flow regimes/patterns are affected by the interplay of the gravity, surface tension and the shear (inertia) forces. The relative magnitude of the forces is clearly affected by the absolute/hydraulic diameter of the tube cross section as well as the shape. Thus it is expected that the sharp corners of a square cross section would allow liquid to be readily trapped along the wetted perimeter. This may allow slug and annular flows to be sustained at higher liquid and gas superficial velocities [5]. A typical interface perturbation of a given magnitude will affect the square cross section and circular cross section in a different manner thus affecting Kelvin-Helmholtz type instabilities and flooding/bridging phenomena.

The above noted peculiarities of a sharp angled PHP were also partly observed by Khandekar et al. [4]. These are decisively confirmed by the results of the present study.

### 3.2 Effect of filling ratio and applied heat load

The two parameters, i.e. filling ratio and heat load, cannot be dealt with separately since they simultaneously affect the internal two-phase flow patterns thereby dictating the dominant heat transfer mechanism and thus the performance.

Table 1 below summarizes the effect of the filling ratio for the present study. The performance is divided into four major operating zones. The effect of heat input on these operating zones is separately highlighted in Table 2. It is difficult to provide a comprehensive description of the effect for each combination of conditions (filling ratio, heat input, inclination angle, flow patterns), but these tables should be taken in the spirit of ‘macro’, broad based operational behavior.

**Table 1: Effect of filling ratio**

FR (%)	Bottom heat mode	Horizontal heat mode	Top heat mode	Zone
0	Empty plate, heat transfer only by conduction			
10	√	X	X	I
20	√	X	X	
30	√	√x	X	II
40	√	√	X	
50	√	√	√	III
60	√	√	√	
70	√	√	√	
80	√	√x	X	IV
90	√	√x	X	
100	Single phase liquid thermosyphon, heat transfer only by natural convection			

**Table 2: Effect of heat load**

Heat (W)	Zone I			Zone II			Zone III			Zone IV		
	B	H	T	B	H	T	B	H	T	B	H	T
<50	√	X	X	√x	√x	X	X	X	X	X	X	X
50	√	X	X	√	√x	X	√	√x	X	√x	√x	X
100	√	X	X	√	√	X	√	√	√	√	√x	X
150	√	X	X	√	√	X	√	√	√	√	√x	X
200	√	X	X	√	√	X	√	√	√	√	√x	X
250	√	X	X	√	√	X	√	√	√	√	√x	X
300	#	X	X	√	√	X	√	√	√	√	√x	X
350	#	X	X	√	X	X	√	√	√	»	√x	X
400	#	X	X	√	X	X	√	√	√	»	√x	X
450	#	X	X	√	X	X	√	√	√	»	√x	X

Index	
<b>B H T</b>	Bottom heat, Horizontal and Top heat mode
√	Operation possible
X	Operation not possible
√x	Intermittent operation, no guarantee
#	Dry-out observed
»	Operation possible, no dry-out observed but $T_e > 100^\circ\text{C}$ , therefore experiment stopped

#### 3.2.1 Working Zone I

Thermal resistance for the dry device is  $\approx 3$  K/W. When the filling ratio is low ( $< \approx 20\%$ ), the plate behaves as an interconnected array of two-phase thermosyphons. Obviously, it can only operate in the bottom heat mode. This operation mode is unique to the sharp angled cross section and was not distinctly observed in previous studies with circular cross section PHPs [6, 7]. The reasons have been explained in the previous section.

Figure 3, captures the details of the flow pattern in

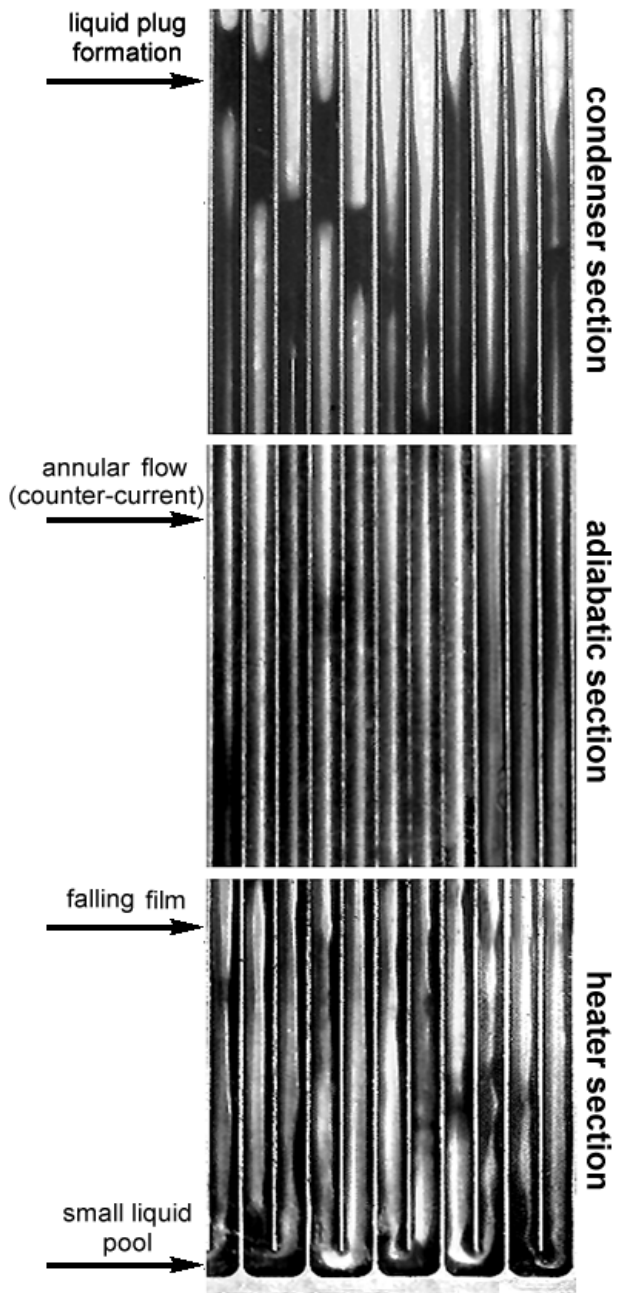


Figure 3: Thermosyphon mode of CLPHP operation in bottom heat mode (FR = 15%)

this mode of operation. It is clear from the picture that the operation is similar to an interconnected array of two-phase thermosyphons. Application of heat results in a 'nucleate pool boiling' type scenario in the individual evaporator U-turns. Slowly, counter-current annular flow develops in individual channels. Vapor flows upwards in every channel and condensate flows down in ripple/rivulet flow. As the vapor condenses, sometimes flooding/bridging is observed resulting in the formation of distinct liquid plugs. These slugs eventually drain down the channel walls through the sharp angled corners. Thus, a counter-current flow is well established. There are little observable pulsations/ oscillations although intermittently instabilities are observed due to the interconnected nature of the thermosyphon array. As the heat load is further increased, the device tends towards a dry-out.

### 3.2.2 Working zone II:

This zone with  $FR \approx 20\%$  to  $40\%$  represents the transition from classical thermosyphon mode to pulsating capillary slug flow regime. The fluid starts migrating to adjacent channels and well defined counter-current flow tends to get disrupted due to the presence of more liquid plugs. Increase in filling ratio will further reduce the thermosyphon effect. The plate can operate well both in the bottom heat and horizontal heat mode, but almost cannot operate in the top heat mode.

In the case of bottom heat mode, the flow pattern is a mixture of classical thermosyphon counter current annular flow and capillary slug flow. There are instances when condensate return is seen as liquid thin film flowing downwards. In addition, there is also a sustained period of capillary slug flow. Thus, a combination of flow patterns exists.

In contrast, in the case of horizontal heat mode, the only dominant flow regime is capillary slug flow, The plug/bubbles primarily oscillate in individual channels of the device.

### 3.2.3 Working zone III:

When the filling ratio is between  $50\%$  and  $70\%$ , the plate can operate rather well at all inclination angles. The effect of the gravity vector becomes relatively insignificant. This zone represents the true pulsating heat pipe operation and is the most effective zone with respect to the thermal performance.

Oscillating slug flow is the predominant flow pattern for horizontal and anti-gravity operation, irrespective of the heat input. The oscillating slug flow gets intermittently superimposed by bulk circulation of the fluid. This bulk circulation happens more and more as heat load is increased thereby reducing the thermal resistance. At small heat loads individual liquid plugs only oscillate about a mean position along the channel length. There is little plug agglomeration.

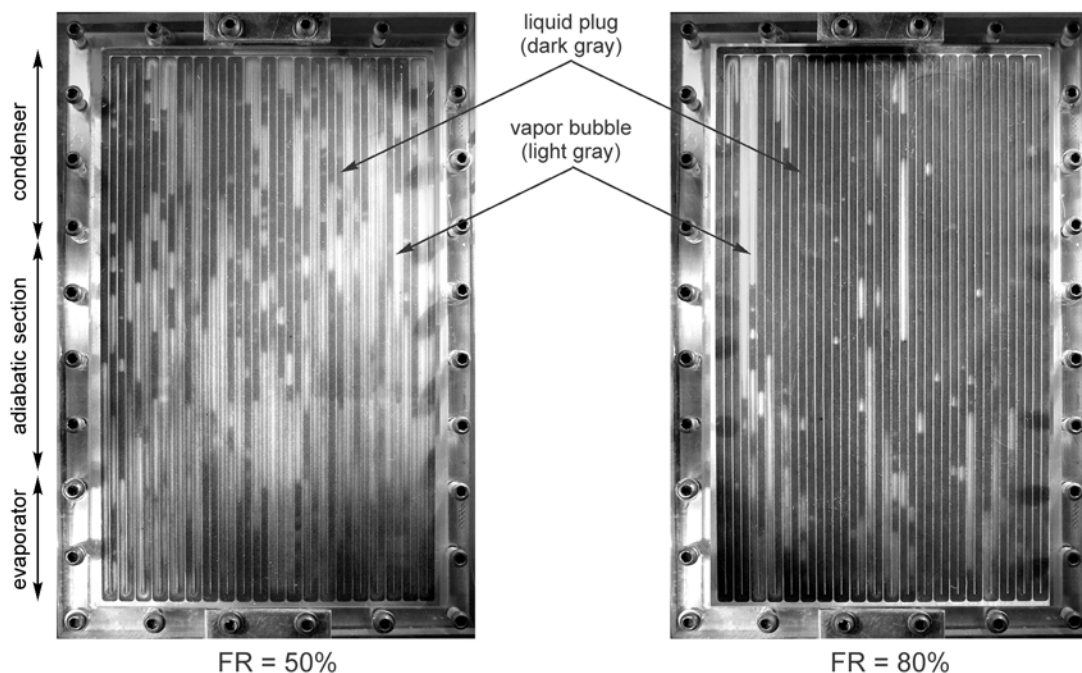


Figure 4 a, b: Photographs of the plate PHP at 200 W heat input power and bottom heat mode

The flow pattern in the bottom heat mode is the most affected by the heat input. At low heat inputs, the flow pattern is predominantly oscillating slug flow and the evaporator temperature somewhat fluctuates. There are periods in which the fluid movement drastically reduces and then all of a sudden there are violent oscillations coupled with bulk circulation which cools the evaporator. Increasing the heat input further smoothens the operation as the evaporator experiences convective boiling leading to churn, semi-annular and annular flow in many channels. Bulk circulation is also superimposed. These combinations of events increase the local heat transfer coefficient and the performance is most desirable in such a situation. A typical snap-shot of a 50% filled device in such an operating mode is shown in Figure 4, a.

### 3.2.4 Working zone IV:

When filling ratio is more than 70%, there is excess liquid which reduces the degree of freedom and the effective advantage of the sharp angled corners. It is almost impossible for the vapor to reach the condenser area unhindered. A typical snap-shot of a 80% filled device operating in bottom heat mode is shown in Figure 4, b. Oscillating/ pulsating action markedly decreases and even disappears for extended time periods. The plate cannot operate in the top heat mode. If the plate can operate in the horizontal heat mode (normally, operation is not always guaranteed), oscillating slug flow is the only flow pattern. In the case of bottom heat mode, nucleate boiling also occurs in the evaporator section, resulting in the formation of small bubbles. The degree of fluid oscillations is the maximum in the bottom heat mode. Still, the overall operation is not quite satisfactory.

For FR = 100% the system works as a single phase thermosyphon [7, 8]. For the present experiment it was not possible to fill it 100% due to flashing.

### 3.3 Quantitative results

Figure 5 shows the thermal performance in terms of effective thermal resistance which is defined as the ratio of the temperature difference between the evaporator and the condenser to the net heat throughput of the system.

In bottom heat mode at low heat input, two local minima are observed. The first at about 15% filling ratio comes under Zone I and corresponds to the thermosyphon effect of the structure. The sharp angled corners produce capillary effects which

enhances the thermosyphon effect. As the heat input is increased, Zone I action terminates due to thermosyphon dryout. The second minimum corresponds to the Zone III. Here, the combined effect of bubble pumping coupled with favorable flow pattern governs the heat transfer. It is worth noting that, on one hand, the thermal resistance in Zone I (thermosyphon mode) is smaller than that in Zone III but on the other hand, maximum heat throughput in this zone is restricted by counter current flow limitation leading to eventual dry-out. As can be clearly seen, the parametric sensitivity of filling ratio gets reduced as the heat load increases. Similar trends are recorded for horizontal heat mode also. For top heat mode, the device can only operate in Zone III.

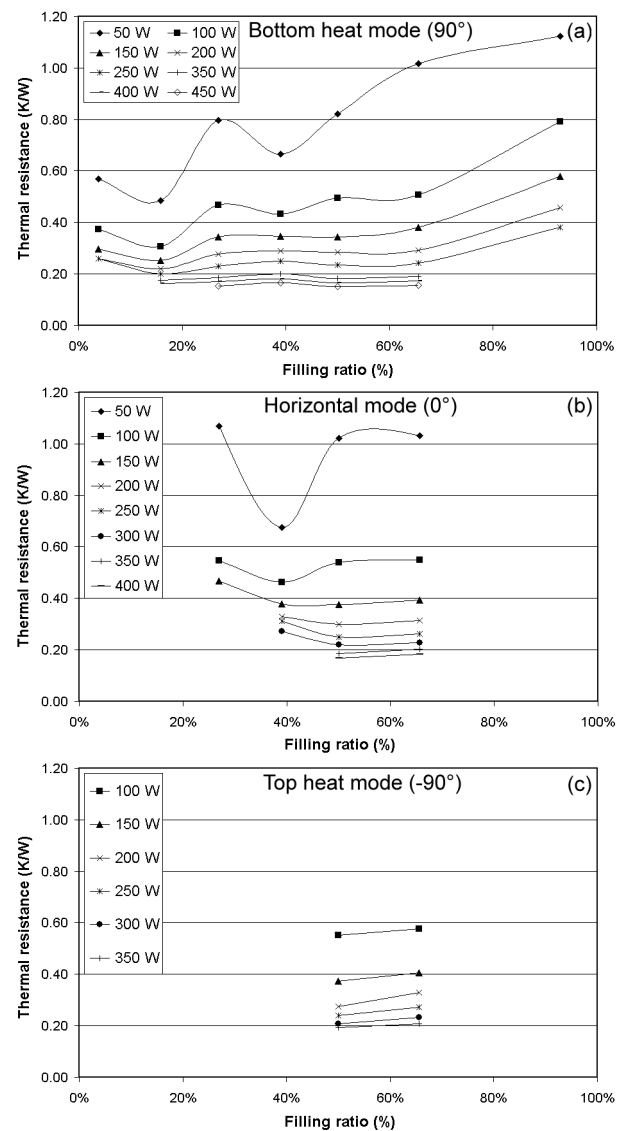


Figure 5: Effect of filling ratio on the thermal resistance of the tested structure (a) bottom heat mode (b) horizontal mode (c) top heat mode

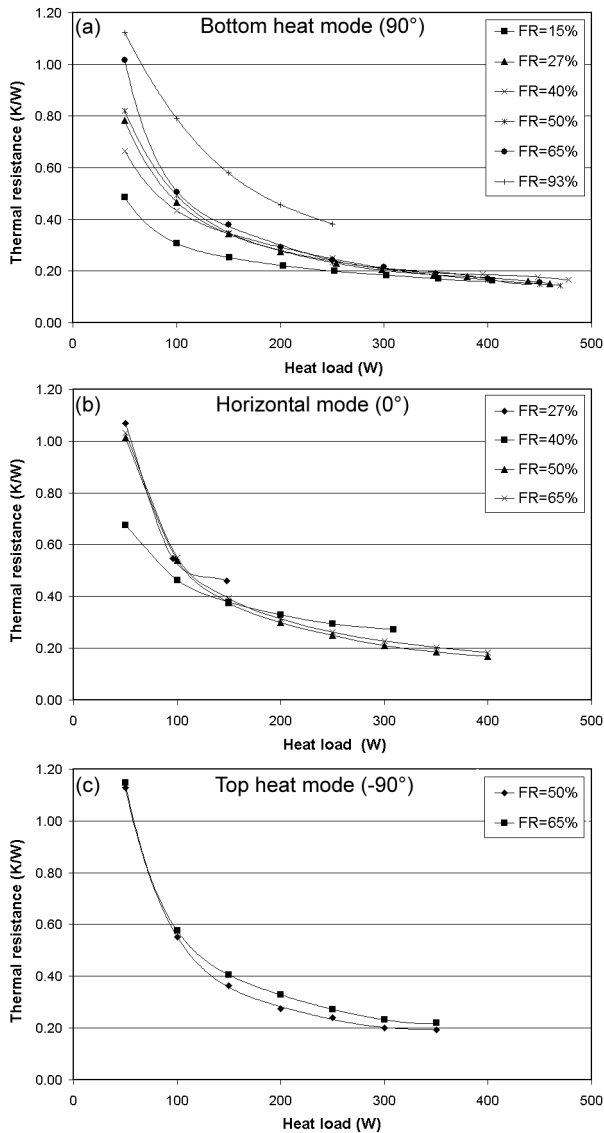


Figure 6: Effect of heat flux on the thermal resistance of the tested structure (a) bottom heat mode (b) horizontal mode (c) top heat mode

Figure 6 depicts essentially the same data points as Figure 5 but is presented here for clarity and better perspective. It shows the effect of heat input on the thermal resistance. It is found that increasing heat load markedly improves the thermal performance. Till about 200 W input power the performance improvement is quite drastic while thereafter it is mild. This tendency is the same for all filling ratios and inclination angles. Overall, the trends are similar to other studies [9, 10]

In general, the heat input is the ‘pump’ for the thermo-fluidic action. Thus increasing the ‘pumping power’ increases the performance. At low filling ratios (Zone I-Thermosyphon mode and Zone II-Transition zone), increasing the heat input makes the liquid layer in the counter-current flow

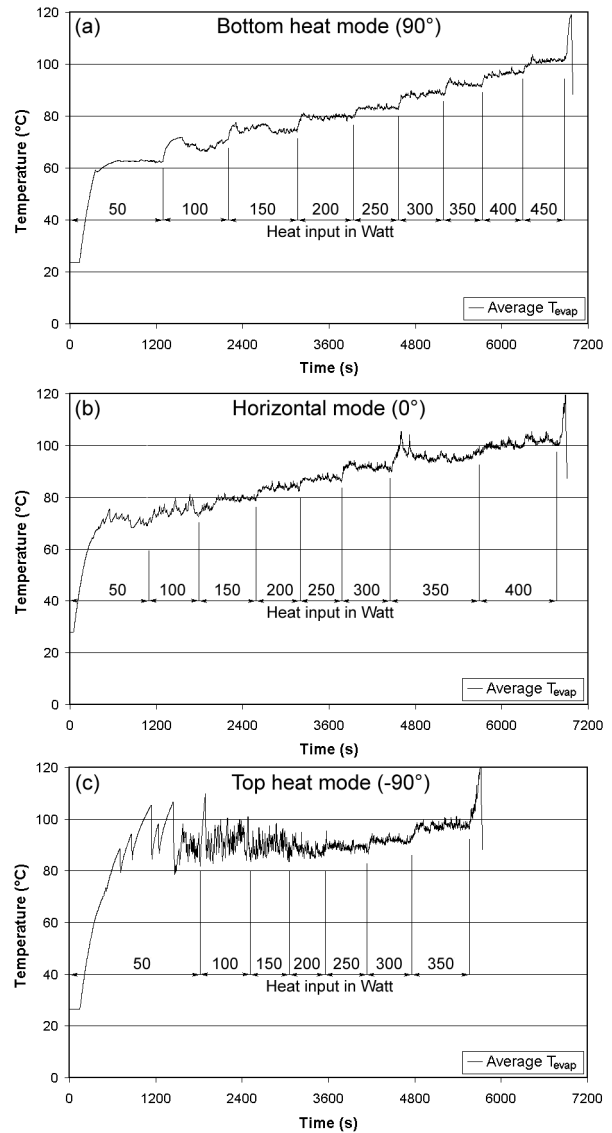


Figure 7: Variation of average evaporator temperature with time (a) bottom heat mode (b) horizontal mode (c) top heat mode

thinner. The effective fluid velocity also increases thus enhancing the local wall heat transfer coefficient. In Zone III operation, bubble pumping action gets enhanced due to rapid bubble growth. Also, after a certain heat input, the flow changes from purely capillary slug flow to churn/ semi-annular and sometimes to fully annular flow in individual channels. This greatly enhances the heat transfer coefficient. Thus, increasing heat load will enhance the performance till a certain type of dry-out occurs. In Zone I, the dryout occurred as a combination of counter-current flow limitation and insufficient fluid inventory, starving some channels completely. In other zones, no dry-out could be observed. Experiments were terminated for safety reasons beyond 120°C local temperatures.

Figure 7 depicts the typical temperature-time history for the average evaporator temperature at FR = 50%, under different operating conditions.

The fluctuations in the evaporator are the minimum for the bottom heat mode. The amplitude increases as the inclination angle changes to horizontal and then to the top heat mode. Overall smoother operation is obtained at higher heat loads. Unacceptable variations are recorded at relatively low heat input in top heat mode. The reasons for this are directly attributed to the mechanisms governing the device operation as explained in Section 3.2.

#### 4 SUMMARY AND CONCLUSIONS

An experimental study with visualization has been performed on a flat plate closed loop pulsating heat pipe having 2 mm<sup>2</sup> square channels. The sharp-angled corners of the cross section render the operational characteristics different from circular cross section devices. Two-phase thermosyphon mode of operation has been clearly observed at low filling ratios. This mode of operation is supported by fluid flow in the sharp angled corners of the channels. The hydraulic diameter does not give the correct critical diameter governed by the Bond number criterion ( $Bo_{crit} \leq 2$ ).

A combination of filling ratio and heat load dramatically affects the thermal performance of the device. These two parameters give rise to a series of possibilities, viz. thermosyphon action, transition from thermosyphon to pulsating action, purely oscillating/ pulsating action, various flow patterns, nucleate and convective flow boiling/condensation scenarios, etc. The device operates with a very low thermal resistance in all operating orientations when the filling ratio is between about 45% and 65% and the heat load is not very low. The effect of gravity then becomes rather insignificant. The very fact that the device can operate in all orientations clearly shows that gravity force is not the only driving force.

#### ACKNOWLEDGEMENTS

The work is partly supported by Deutsche Forschungsgemeinschaft (DFG) under Grant GR-412/33-1. The financial support from DAAD (Deutscher Akademischer Austauschdienst) for the doctoral study of Ms. Honghai Yang is greatly appreciated.

#### NOMENCLATURE

Bo : Bond number =  $D \cdot [g(\rho_{liq} - \rho_{vap}) / \sigma]^{0.5}$   
D : diameter (m)  
FR : filling ratio ( $V_{liq}/V_{tot}$ )  
T : temperature (°C)  
V : volume (m<sup>3</sup>)  
g : acceleration due to gravity (m/s<sup>2</sup>)

Greek Symbols:

$\sigma$  : surface tension (N/m)  
 $\rho$  : density (kg/m<sup>3</sup>)

Subscripts

evap : evaporator  
crit : critical  
liq : liquid  
tot : total  
vap : vapor

#### REFERENCES

1. Akachi H., US patent, Number 5219020, 1993.
2. Akachi H., US patent, Number 5490558, 1996.
3. Akachi H., Polášek F. and Štulc P., Pulsating Heat Pipes, Proc. 5th Int. Heat Pipe Symp., Melbourne, pp. 208-217, 1996.
4. Khandekar S., Schneider M., Schäfer P., Kulenovic R. and Groll M., Thermofluiddynamic Study of Flat Plate Closed Loop Pulsating Heat Pipes, Microscale Thermophysical Engg., Vol. 6/4, pp. 303-318, 2002.
5. Coleman J. and Garimella S., Characterization of Two-phase Flow Patterns in Small Diameter Round and Rectangular Tubes, Int. J. Heat and Mass Transfer, Vol. 42, pp. 2869-2881, 2004.
6. Khandekar S., Dollinger N. and Groll M., Understanding Operational Regimes of Pulsating Heat Pipes: An Experimental Study, Applied Thermal Engg., Vol. 23/6, pp. 707-719, 2003.
7. Groll M. and Khandekar S., Pulsating Heat Pipes: Progress and Prospects, Proc. 3rd Int. Conf. on Energy & Environment, ISBN 7-5323-7335-5/TK-22, Vol. 1, pp. 723-730, Shanghai, China, 2003.
8. Khandekar S., Groll M., Charoensawan P. and Terdtoon P., Pulsating Heat Pipes: Thermo-fluidic Characteristics and Comparative Study with Single Phase Thermosyphon, Proc. 12th Int. Heat Transfer Conf., ISBN-2-84299-307-1, Vol. 4, pp. 459-464, Grenoble, France, 2002.
9. Qu W. and Ma T., Experimental Investigation on Flow and Heat Transfer of a Pulsating Heat Pipe, Proc. 12. Int. Heat Pipe Conf., pp. 226-231, Moscow, 2002.
10. Khandekar S. and Groll M., An Insight into Thermo-Hydraulic Coupling in Pulsating Heat Pipes, Int. J. of Thermal Sciences (Rev. Gén. Therm.), Elsevier Science, ISSN: 1290-0729, Vol. 43/1, pp. 13-20, 2004.